DMD Fast Forward. Published on April 20, 2005 as doi:10.1124/dmd.104.002998

DMD 2998R

IDENTIFICATION OF CYTOCHROME P450 AND ARYLAMINE N-ACETYLTRANSFERASE ISOFORMS INVOLVED IN SULFADIAZINE METABOLISM

Helen R. Winter and Jashvant D. Unadkat[1]

Department of Pharmaceutics, University of Washington, Seattle, Washington (J.D.U.)

Current affiliation: AstraZeneca LP, Wilmington, Delaware (H.R.W.)

Running Title: **P450 and NAT involvement in sulfadiazine metabolism**

Correspondence should be addressed to:

Jashvant D. Unadkat, Department of Pharmaceutics, Box 357610, University of Washington, Seattle WA 98195 USA

Fax: (206) 543-3204 Tel: (206) 543-9434

EMAIL: jash@u.washington.edu

Text pages: 16

Tables: 1

Figures: 8

References: 34

Abstract: 248

Introduction: 398

Discussion: 968

Abbreviations: DDC, diethyldithiocarbamate; DL-DTT, DL-dithiothreitol; EC, electrochemical; EDTA, ethylenediaminetetraacetic acid; HLM, human liver microsomes; HLC, human liver cytosol; HPLC, high performance liquid chromatography; NAT, arylamine N-acetyl transferase; PABA, p-amino benzoic acid; SMZ, sulfamethazine; SDZ, sulfadiazine; SDZ-HA, N-hydroxy sulfadiazine; AcSDZ, acetyl sulfadiazine

ABSTRACT

Sulfadiazine hydroxylamine has been postulated to be the mediator of the greatly increased rates of adverse reactions to sulfadiazine experienced by people with HIV infection. Therefore, we investigated the in vitro human cytochrome P450 (CYP) and N-arylamine acetyltransferase (detoxification) metabolism of sulfadiazine. Formation of both the hydroxylamine and 4-hydroxy sulfadiazine was NADPH-dependent in human liver microsomes (HLM). The average Km (± SD) and Vmax in HLM (n = 3) for hydroxylamine formation was 5.7 ± 2.2 mM and 185 ± 142 pmol/min/mg, respectively. Significant ($p < 0.05$) inhibition by selective CYP isoform inhibitor sulfaphenazole (2.1 μM, CYP2C9) indicated a role for CYP2C9 in the formation of the hydroxylamine. Hydroxylamine formation correlated strongly with tolbutamide 4-hydroxylation (CYP2C8/9) in HLM (r = 0.76, $p \leq 0.004$, n = 12). Fluconazole (CYP2C9/19 and CYP3A4 inhibitor at clinical concentrations) inhibited hydroxylamine formation, with one-enzyme model Ki estimates ranging from 9 to 40 μM. Acetylation of sulfadiazine in human liver cytosol (HLC) correlated strongly with NAT2 activity as measured by sulfamethazine N-acetylation (r = 0.92, $p < 0.001$, n = 12). The average Km (± SD) and Vmax in HLC (n = 3) was 3.1 ± 1.7 mM and 221.8 ± 132.3 pmol/min/mg, respectively. The polymorphic acetylation of sulfadiazine may predispose slow acetylator patients to adverse reactions to sulfadiazine. On the basis of our Ki estimates, clinical fluconazole concentrations of 25 μM would produce decreases of 40 to 70% in hepatic mediated hydroxylamine production. Therefore, we predict that fluconazole may prove useful in the clinic as an in vivo inhibitor of sulfadiazine hydroxylamine formation to suppress adverse reactions to this drug.

Sulfadiazine has an important role in acute therapy for *Toxoplasmosis gondii* encephalitis, the most common opportunistic infection of the brain experienced by AIDS patients. Sulfadiazine is an arylamine antibiotic associated with an extraordinarily high rate of adverse reactions, ~40% in AIDS patients (Haverkos et al., 1987; Leport et al., 1988). Typical doses for toxoplasmic encephalitis in AIDS patients are high and range up to 8 g administered daily in four divided doses. Some of the adverse effects of arylamines are thought to be caused by formation of the hydroxylamine metabolite that is further oxidized to the highly electrophilic nitroso metabolite, which covalently binds to cellular macromolecules resulting in adverse reactions (Shear and Spielberg, 1985; Reider et al., 1988). Although sulfadiazine has been marketed since the 1940s, very little is known about cytochrome P450 isoform involvement in hydroxylamine formation in humans or the arylamine N-acetyltransferase (NAT) detoxification pathway. The only oxidative metabolite previously reported in humans was 4-hydroxy sulfadiazine, which comprised 12% of the dose in a slow acetylator (Vree et al., 1995). The 5-hydroxy sulfadiazine metabolite has been identified in monkeys (Vree et al., 1995), and the 4-hydroxy, 5-hydroxy and dihydroxy sulfadiazine metabolites have been identified in various animal species (Atef 1974; Nouws et al., 1987, 1988; Vree et al., 1991a, 1991b). Leone et al. (1987) reported that 30 to 60% of a dose of sulfadiazine is eliminated as the parent and 20 to 40% is eliminated as the acetylated metabolite in humans. Sulfadiazine plasma Cmax concentrations following a single 2-g oral dose of sulfadiazine are predicted to be 300 μg/ml or 1.2 mM (Vree et al., 1995).

Human arylamine N-acetyl transferase (NAT) is encoded at two different loci. The enzyme encoded at one locus has a wide tissue distribution, is responsible for acetylation of ρ-amino benzoic acid (PABA) and is termed NAT1. The second locus encodes an enzyme, which has a more restrictive tissue distribution with higher levels of expression in the liver and red blood

cells, is responsible for the acetylation of sulfamethazine (SMZ) and is termed NAT2. NAT2 is associated with the classic form of human NAT polymorphism. Both NAT1 and NAT2 genes have allelic variation (Butcher et al., 2002). Slow acetylator status has been associated with increased rates of adverse reactions to arylamine antibiotics, such as sulfamethoxazole (Wolkenstein et al., 1995). Suppression of hydroxylamine formation through the use of metabolic inhibitors has been explored as a therapeutic strategy to decrease the high rate of adverse reactions to the arylamines dapsone (Mitra et al., 1995, Winter et al., 2004a) and sulfamethoxazole (Mitra et al., 1996, Winter et al., 2004b) in people with AIDS.

The major aim of this study was to identify the cytochrome P450 isoforms involved in sulfadiazine hydroxylation in order to identify potentially clinically useful in vivo inhibitors of this pathway. A secondary aim was to determine which NAT enzyme(s) was responsible for sulfadiazine acetylation.

Materials and Methods

Chemicals. 4-hydroxy sulfadiazine, 5-hydroxy sulfadiazine, N-hydroxy sulfadiazine (the hydroxylamine), and N-acetyl sulfadiazine were obtained from the National Institute of Allergy and Infectious Diseases AIDS Research and Reference Reagent Program. Sulfadiazine was purchased from Sigma Chemical (St. Louis, MO). N-acetyl sulfamethazine was a gift from Dr. Edith Sim, University of Oxford, and N-acetyl ρ-aminobenzoic acid was obtained from Aldrich Chemical (Milwaukee, WI). All other chemicals were of analytical grade and were obtained commercially.

Human Liver Samples. Livers were procured, processed, and stored as previously described (Rettie et al., 1989). Microsomes (HL123, 126, 135, 141, and 142) were prepared as previously described (Hickman et al., 1998). Cytosol was prepared by homogenizing human liver in a

buffer containing 250 mM sucrose, 100 mM dihydrogen potassium phosphate, 1 mM EDTA, 1 μg/ml leupeptin, and 1 mM DTT at pH 7.4. The liver homogenate was centrifuged at 15,000g at 4°C for 20 min, and the supernatant was poured through two layers of gauze into fresh centrifuge tubes and then centrifuged at 100,000g at 4°C for 1 h to isolate the cytosol as the supernatant. The supernatant was aliquoted immediately, then frozen in liquid nitrogen before storing at -70°C. Protein concentrations were determined by the Bradford assay with bovine serum albumin standard supplied by Biorad (Hercules, CA).

Cloned Human Enzymes. Lymphoblast and baculovirus insect cell-expressed (Supersome™) human cytochrome P450 enzymes were obtained from Gentest® (Woburn, USA). Bacterially expressed NAT1*3 and NAT2*4 (both the human wild-type) were provided by Dr. Dean Hickman and have been previously characterized and described by Palamanda and colleagues (1995).

Stock Preparation. Sulfadiazine hydroxylamine was dissolved in argon-purged dimethyl sulfoxide (DMSO) in gas-tight amber autosampler vials into which freshly prepared aqueous 10 mM ascorbic acid (10% vol/vol) was injected. The head-space of the gas-tight vials was purged with argon, and the vials were kept on ice or stored at -70°C. All dilutions were made in freshly prepared 10 mM ascorbic acid using gas-tight syringes and liquid-to-liquid transfer techniques. All other stocks were prepared as equimolar sodium salts and freshly diluted in buffer, pH 7.4 at 37°C.

Cytochrome P450 Assays. *HPLC assay.* The analytical system consisted of a Coulochem II™ electrochemical detector (EC) (G = 200 mV, E1 = 100 mV, E2 = -200 mV) coupled to a downstream Shimadzu SPD-6A UV detector (λ = 266 nm). Optimal Coulochem performance required a Shimadzu LC600 dual piston pump coupled to an Alltech Free Flow Pulse

Dampener™ and a Spectraphysics SP8875 autosampler using a Rheodyne® injector valve. A C18 reverse phase column (Ultrasphere, 4µ, 250 x 4.6 mm, Beckman Instruments, Fullerton, CA) was used with a mobile phase consisting of 5: 0.05: 95 (vol/vol) acetonitrile/triethylamine/ 50mM sodium citrate, 1 mM EDTA, pH 2.21, at a flow rate of 1 ml/min. EC detection was used for the hydroxylamine, and UV detection was used for all other metabolites of interest.

Enzyme assays. The 250 µl microsomal incubation matrix consisted of 0.1 to 2 mg/ml microsomal protein, 1 mM EDTA, and 1 mM glutathione in 50 mM HEPES buffer, pH 7.4 at 37°C. All inhibitors were prepared as aqueous solutions unless specified. The final concentration of organic solvent in the incubation mix did not exceed 1% (vol/vol). Incubations for mechanism-based inhibitors, such as troleandomycin and diethyldithiocarbamate (DDC), were carried out as described by Hickman and colleagues (1998). Reactions were pre-incubated for 5 min; then 1mM NADPH was added, and the reaction was terminated after 5 to 10 min with 25 µl 2N HCl or 1.5 % perchloric acid. Samples were vortexed under an atmosphere of argon, left on ice for 10 min, and centrifuged at 20,000g at 4°C for 10 min; then the supernatant was injected into pre-assembled argon-purged, gas-tight amber autosampler vials. Samples were injected onto the HPLC within 3 h of the incubation.

Arylamine N-Acetyltransferase Assays. *HPLC assays.* The analytical system described above was used for the analysis of N-acetylated sulfadiazine with UV detection at 266 nm. The mobile phase consisted of 10: 0.05: 90 (vol/vol) acetonitrile/triethylamine/acetic acid at a flow rate of 1 ml/min.

Enzyme assays. Assays were conducted by the method reported by Grant and colleagues (1991). Acetyl coenzyme A concentrations were fixed at 100 µM. Incubations contained 40 µl of liver cytosol diluted to the appropriate concentration with 250 mM sucrose; 20 µl of acetyl-DL-

DMD Fast Forward. Published on April 20, 2005 as DOI: 10.1124/dmd.104.002998
This article has not been copyedited and formatted. The final version may differ from this version.

carnitine/carnitine acetyl transferase cofactor regenerating system dissolved in 225 mM triethanolamine-HCl , 4.5 mM DL-DTT, pH 7.5; 20 µl of acetyl coenzyme A (450 µM in water); and varying amounts of sulfadiazine, sulfamethazine, or para amino benzoic acid diluted as its sodium salt in TRIS 20 mM buffer to start reactions. Reactions were terminated with 10µl of 15% perchloric acid and 50 µl injected onto the HPLC.

Data Analysis. Apparent IC_{50} ($IC_{50,\,app}$) and residual effect model IC_{50} ($IC_{50,\,rem}$) estimates were obtained from probit plots and nonlinear regression estimation using the equation below:

$$\%\ \text{Control activity} = E\max - (E\max - E0) * \left(\frac{I}{(I + IC_{50,\,rem})}\right) \text{.-(1)}$$

where Emax was the maximal rate of hydroxylamine production in the absence of inhibitor, E0 was the un-inhibitable hydroxylamine production rate, and I was the inhibitor concentration. To determine $IC_{50,\,app}$, E0 was assumed to be zero. Initial estimates of Ki (inhibitor binding affinity for the enzyme) were obtained from Dixon plots, and the mechanism of inhibition was confirmed by Lineweaver-Burk transformation. Nonlinear regression estimation of IC_{50} and Ki for one-enzyme models of inhibition was performed using PCnonlin (Scientific Consulting, Apex, NC) and reported as the parameter ± SEM.

Nonlinear regression estimation of parameters for two-enzyme models where only one enzyme was competitively (2) or noncompetitively (3) inhibited by fluconazole were also performed using the equations below:

$$V = \frac{S * V\max_1}{S + Km_1 * (1 + I/Ki)} + \frac{S * V\max_2}{S + Km_2} \text{ -(2)}$$

$$V = \frac{S * V\,max_1}{S * (1 + I/Ki) + Km_1 * (1 + I/Ki)} + \frac{S * V\,max_2}{S + Km_2} \quad -(3)$$

where V was the rate of hydroxylamine formation; Vmax(n), the maximal rate of hydroxylamine formation for each enzyme (n) and Km(n), a measure of substrate affinity and the substrate concentration (S) that produces Vmax(n)/2.

All statistical data are reported as the mean ± SD of triplicate determinations. The unpaired *t* test was used to detect significant differences ($p \leq 0.05$). The Pearson correlation coefficient (r) and the Spearman rank correlation coefficient (r_s) were used to determine the significance of substrate and isoform selective probe activity correlations. The *F*-ratio test was used to discriminate between one- and two-enzyme inhibition models.

Results

Cytochrome P450 Assays. *HPLC sulfadiazine oxidative metabolite assay development.* Oxidation potentials for the hydroxylamine and 5-hydroxy sulfadiazine were 0 and 400 mV, respectively. Oxidation potentials for 4-hydroxy sulfadiazine, N-acetyl sulfadiazine, and sulfadiazine were greater than 600 mV. Because EDTA in the mobile phase becomes significantly oxidized at 400 mV, electrochemical detection at E1 = 100 mV was used only for the hydroxylamine. When there were significant interfering peaks in the chromatography, the response to reduction of the nitroso species (oxidative product of the hydroxylamine) was monitored with E2 = -200 mV, which was immediately downstream from E1. UV detection at 266 nm was used for all of the other metabolites of interest. Sample chromatograms where 4-hydroxy sulfadiazine, N-hydroxy sulfadiazine, 5-hydroxy sulfadiazine, and sulfadiazine eluted at 8.4, 10.2, 11.9, and 12.8 min, respectively, are shown in Fig. 1.

The limit of detection for the hydroxylamine in the microsomal sample matrix was less than 0.2 pmol on column, and calibrations were linear over the range 0.2 to 2 pmol injected on column with $r^2 = 0.998$. The accuracy and precision for the assay of the hydroxylamine were typically less than 6.1 and 16.8%, respectively. 4-hydroxy and 5-hydroxy sulfadiazine calibrations were linear over the range of 4 to 75 pmol injected on column with $r^2 \geq 0.99$.

Determining linear conditions and parameters for Michaelis-Menten kinetics. The hydroxylamine was stable for only 15 min (10% loss) in the full sample matrix containing heat de-natured protein at 37°C. The hydroxylamine spiked into the full sample matrix treated with 0.2N HCl was stable for greater than 6 h in argon-purged gas-tight autosampler vials.

The hydroxylamine and 4-hydroxy sulfadiazine were produced in human liver microsomes in a reaction that required NADPH, and their formation was eliminated by the presence of 1% triton, indicating a role for cytochrome P450 metabolism. Formation of 5-hydroxy sulfadiazine was not detected in human liver microsomes. Formation of the hydroxylamine and 4-hydroxy sulfadiazine was linear up to 15 and greater than 40 min, respectively, with protein concentrations up to 2 mg/ml. Hydroxylamine formation appeared as uniphasic plots on Eadie-Hofstee plots (Fig. 2) with an average Km (± SD) of 5.7 ± 2.2 mM and seven-fold variation in Vmax of 185 ± 142 pmol/min/mg protein. Formation of 4-hydroxy sulfadiazine in HL123 had an apparent Km > 10 mM with a formation rate of 69.2 pmol/min/mg protein at 10mM sulfadiazine. The limited solubility of sulfadiazine in the microsomal incubation matrix (10 mM) did not allow us to determine the Km for 4-hydroxy sulfadiazine formation with confidence.

DMD Fast Forward. Published on April 20, 2005 as DOI: 10.1124/dmd.104.002998
This article has not been copyedited and formatted. The final version may differ from this version.

Isoform selective inhibition screening of hydroxylamine formation. Screening with cytochrome P450 isoform selective inhibitors of hydroxylamine formation in human liver microsomes at clinical concentrations of sulfadiazine 100 μM showed significant inhibition by 250 μM tolbutamide (2xKm CYP2C9, Veronese et al., 1993) and 2.16 μM sulfaphenazole (CYP2C9), indicating a role for CYP2C9 ($p \leq 0.05$, see Fig. 3).

Lymphoblast-expressed CYP2C9*1 showed good sulfadiazine hydroxylation activity, with a Km of 7.2 ± 0.3 mM and Vmax of 36.9 ± 1.3 pmol/min/pmol P450. Lymphoblast-expressed CYP2C8 and CYP2C19 had activity that was 5 to 7 times greater than the vector control enzyme at 5 mM sulfadiazine. Baculovirus insect cell-expressed CYP2C8 (Supersomes™) without co-expressed cytochrome b5 had a Km of 2.59 ± 0.06 mM and Vmax of 0.330 ± 0.010 pmol/min/pmol P450. Baculovirus insect cell-expressed CYP2C8 (Supersomes™) with co-expressed cytochrome b5 had a Km of 2.87 ± 0.16 mM and Vmax of 0.571 ± 0.009 pmol/min/pmol P450. CYP2B6 appeared to have Km much greater than 10 mM (rate of hydroxylamine formation at 10mM was 0.41pmol/min/pmol P450). All other lymphoblast-expressed enzymes investigated (CYP1A1, CYP1A2, CYP2A6, CYP2D6, CYP3A4, CYP2E1) did not show activity significantly greater than the endogenous activity of the control. A role for CYP2C8/9 in hydroxylamine formation was indicated by a strong correlation between the rate of sulfadiazine hydroxylamine formation (4 mM) and 4-hydroxylation of tolbutamide (500 μM) for 12 human livers (Fig. 4; $r = 0.76$, $p < 0.004$; $r_s = 0.78$, $p < 0.002$).

Fluconazole as a selective inhibitor of hydroxylamine formation. Fluconazole, an inhibitor of CYP2C9/19 and CYP3A4 at clinical concentrations, was investigated as a selective inhibitor of hydroxylamine formation. The $IC_{50,\,app}$ for fluconazole (0-200 μM) at a sulfadiazine

concentration of 100 μM in three livers (HL123, HL141, and HL142) was 32.0 ± 13.7 μM (16.2 to 40 μM). The $IC_{50, rem}$ was 11.7 ± 2.0 μM (9.5 to 13.3 μM), with residual activity of 25.7 ± 7.4% (17.2 to 30.0%). The significant residual activity indicated the presence of at least two enzymes in hydroxylamine formation, therefore, nonlinear regression analysis was used to determine the fluconazole Ki for one and two enzyme models of inhibition. For the one-enzyme models, the fluconazole Ki in HL142 was determined to be 8.6 ± 0.6 μM with a competitive mechanism, and the Ki in HL123 was 39.5 ± 2.8 μM with a noncompetitive mechanism, as shown by Dixon and Lineweaver-Burk plots in Fig. 5. However, the subtle non-linearities in the data for HL123 are also consistent with a two-enzyme model in which one enzyme is competitively inhibited by fluconazole, but the other enzyme is not inhibited (Equations 2 and 3). For competitive inhibition of one of the enzymes responsible for hydroxylamine formation in HL123 (enzyme 1), the parameters for Vmax1, Km1, Vmax2, Km2, and the Ki were estimated to be 253 ± 21 pmol/min/mg, 8.6 ± 1.3 mM, 51.3 ± 5.8 pmol/min/mg, 2.1 ± 0.4 mM, and 10.4 ± 2.5 μM, respectively. When simulations were performed for an enzyme model with these parameters, apparent one-enzyme noncompetitive profiles were obtained for both the Dixon and Lineweaver Burk plots (data not shown). The average $IC_{50, rem}$ agrees closely with the Ki obtained for the two-enzyme model for HL123. Km1 for the fluconazole inhibitable enzyme is close to the estimate of 7.2 mM for lymphoblast-expressed CYP2C9, and Km2 is close to the estimate of 2.6 mM and 2.9 mM obtained for baculovirus insect cell-expressed CYP2C8 with and without supplemental cytochrome b5, respectively. The data were also fit to a two-enzyme model in which fluconazole inhibition was noncompetitive for one of the enzymes (Equation 3) with the parameters for Vmax1, Km1, Vmax2, Km2, and the Ki estimated to be 203 ± 18 pmol/min/mg, 6.0 ± 0.9 mM, 71 ± 7 pmol/min/mg, 4.7 ± 0.7 mM, and 16.2 ± 1.1 μM,

respectively. As determined by the *F*-ratio test, both the two-enzyme models (Equations 2 and 3) were a significantly ($p < 0.001$) better fit to HL123 data versus the one-enzyme models. Since fluconazole inhibited the one-enzyme model of HL142 with a competitive mechanism, the two-enzyme competitive model appears to be the model most consistent with our HL123 data.

Arylamine N-Acetyltransferase Assays. *HPLC N-acetyl sulfadiazine metabolite assay development.* Retention times for sulfadiazine and N-acetyl sulfadiazine were 8.0 and 11.5 min, respectively. Calibrations were linear and reproducible over the range of 8.5 to 1000 pmol injected on column ($r^2 \geq 0.992$). Cloned NAT enzymes expressed in E. coli produced a time-dependent interfering peak caused by an interaction between perchloric acid and the bacterial protein. Cloned enzyme incubations were therefore terminated with 90 μL acetonitrile, then diluted to a final concentration of 20% acetonitrile, and the supernatant injected on the HPLC.

Determining linear conditions and parameters for Michaelis-Menten kinetics. Formation of N-acetyl sulfadiazine was linear up to 1 h with cytosolic protein concentrations up to 2 mg/ml. N-acetyl sulfadiazine formation appeared uniphasic on Eadie-Hofstee plots (Fig. 6) with an average Km (± SD) and Vmax of 3.1 ± 1.7 mM and 221.8 ± 132.3 pmol/min/mg, respectively, at an acetyl coenyzme A concentration of 100 μM. Enzyme kinetic parameters for bacterially expressed wild-type NAT1*3 and NAT2*4 are listed in Table 1, where both enzymes had similar Km values of 5.8 ± 0.2 mM and 5.4 ± 0.2 mM, respectively, for sulfadiazine acetylation.

Isoform selective inhibition screening of N-acetyl sulfadiazine formation. Selective inhibition screening in three livers using 250 μM SMZ as the NAT2 probe and 100 μM PABA as the NAT1 probe showed a dominant NAT2 component in two livers and an apparent dominant NAT1 component in one liver (HL142) (Fig. 7). The acetylation of sulfadiazine in 12 human

livers was not correlated with NAT1 activity, as shown by ρ-aminobenzoic acid acetylation, but was correlated with NAT2 activity by sulfamethazine acetylation (Fig. 8; $r = 0.96$, $p < 0.001$; $r_s = 0.92$, $p < 0.001$).

Discussion

We developed a highly sensitive, selective electrochemical HPLC assay that enabled us to detect and quantify the highly unstable hydroxylamine of sulfadiazine. Our human liver microsomal data are consistent with a significant role for cytochrome P450 in both hydroxylamine and 4-hydroxy sulfadiazine formation. Detection of 4-hydroxy sulfadiazine is consistent with a report by Vree and colleagues (1995). Despite the Km for the hydroxylamine being in the millimolar range, the reported recovery of 14% of a sulfadiazine dose as 4-hydroxy sulfadiazine (which appears to have an even higher Km in human liver microsomes) in a slow acetylator (Vree et al., 1995) suggests that hydroxylamine production would be significant in vivo.

The isoform selective screening profile and the correlation of the rate of hydroxylamine formation with tolbutamide 4-hydroxylation strongly indicates a role for CYP2C8/9 in hydroxylamine formation. Tolbutamide 4-hydroxylation has been demonstrated to be a reliable measure both of in vitro and in vivo CYP2C9 activity even when CYP2C9 allelic variants are present (Gill et al., 1999; Kirchheiner et al., 2002; Shon et al., 2002). In support of CYP2C9 involvement is a clinical study in which phenytoin clearance, which is largely CYP2C9-mediated with a minor contribution by CYP2C19 (Levy, 1995), was inhibited significantly (~50%, $n = 8$) by a 4-g oral dose of sulfadiazine (Hansen et al., 1979). When fluconazole (a CYP2C9/19 and CYP3A4 inhibitor at clinical concentrations) was explored as a potentially useful clinical inhibitor of hydroxylamine formation, significant residual enzyme activity ranging from 17.2 to

30% was found, indicating a role for one or more non-fluconazole inhibitable enzymes. The variability in fluconazole $IC_{50,\ app}$ estimates (16.2 to 40 μM) at clinical sulfadiazine concentrations of 100 μM agreed with the variability in the range of Ki values for one-enzyme models (8.6 to 39.5 μM) determined. In a previous study on dapsone hydroxylamine formation (Winter et al., 2000), we found that CYP2C8, unlike other members of the CYP2C family, was not inhibited by fluconazole at concentrations up to 200μM. As sulfaphenazole is not an inhibitor of CYP2C8, our observation that tolbutamide 250 μM (2 × Km of 2C9; Miners et al., 1988) inhibited sulfadiazine hydroxylamine formation greater than sulfaphenazole (18 × Ki of 2C9; Miners et al., 1988) also supports a potential role for CYP2C8 in sulfadiazine hydroxylamine formation (Fig. 3).

The fluconazole $IC_{50,\ rem}$ determined using a residual effect model was 11.7 ± 2 μM (9.5-13.3), which agrees closely with the fluconazole Ki of 8 μM determined for CYP2C9-mediated S-warfarin 7-hydroxylation (Kunze et al., 1996). The Ki for fluconazole inhibition of cloned CYP3A4 has been reported to be 9.21 μM (Gibbs et al., 1998). In the case of sulfadiazine, a major role for CYP3A4 was discounted because of the inhibition screening profile and the undetectable clone enzyme activity. The significant residual activity shown by the fluconazole IC_{50} profiles and the apparently noncompetitive Dixon and Lineweaver profiles for HL123 are completely consistent with a two-enzyme model in which there is competitive inhibition of CYP2C9 and a lack of fluconazole inhibition of CYP2C8 (and/or other enzymes) in hydroxylamine formation. The two-enzyme model with one of the enzymes inhibited competitively by fluconazole is consistent with known CYP2C8 and CYP2C9 interactions with fluconazole. Therefore, this model is considered the most appropriate model to explain the

widely varying IC_{50} and one-enzyme model Ki estimates for fluconazole inhibition of sulfadiazine hydroxylamine formation in human liver microsomes. CYP2C8 content is known to vary widely in human livers (Wrighton et al., 1987) and is resistant to inhibition by fluconazole (Winter et al., 2000). Therefore, this enzyme is likely to be one of the major sources of the variability observed.

Acetylation of sulfadiazine in human liver is mediated by NAT2, as shown by a strong correlation with the NAT2-specific sulfamethazine N-acetylation. Because the bacterially expressed human wild-type NAT enzymes had very similar Km values, the *in vivo* NAT2 enzyme must have much greater activity towards sulfadiazine acetylation, either in the form of a higher catalytic rate constant (kcat) and/or a much greater level of enzyme expression in human liver. Sulfadiazine acetylation would be expected to be a predominantly NAT2-mediated process as sulfamethazine (our NAT2 probe) is actually 4-,6-dimethyl sulfadiazine. Methylation of the para substituent must enhance affinity for NAT2 as the reported Km for sulfamethazine acetylation is only 120 μM (Grant et al., 1991). NAT2 is expressed predominantly in the liver and red blood cells, whereas NAT1 is expressed ubiquitously. It is possible that NAT1-mediated acetylation may predominate in non-hepatic tissues. The Km for sulfadiazine N-acetylation is comparable to that found for hydroxylamine formation. Slow acetylator status may predispose patients to sulfadiazine adverse reactions by allowing more parent drug to be available for oxidative pathways and hydroxylamine formation.

The cause of the extremely high rate of adverse reactions to sulfadiazine and other arylamine drugs, such as sulfamethoxazole and dapsone, in HIV-infected patients has not been determined. If the rate of adverse reactions is related to the total body burden of cytochrome P450-mediated production of the hydroxylamine, then potent inhibitors of CYP2C8/9 activity suitable for use in

the clinic would be predicted to decrease the rate of adverse reactions and allow patients to complete their antibiotic therapy. Inhibition of a metabolite's formation clearance (CLf) by an inhibitor (I) with an in vitro-determined Ki can be predicted for a one-enzyme Michaelis-Menten model based on the following equation derived by Shaw and Houston (1987) for both competitive and noncompetitive mechanisms of inhibition where

$$\frac{Cl,f}{CLf,I} = 1 + \frac{I}{Ki} \quad -(4)$$

assuming that the substrate concentrations are much less than the Km for the enzyme. At expected fluconazole clinical concentrations of 25 μM (Winter et al., 2004a; Winter et al., 2004b) and an observed one-enzyme model Ki range of 8.6 to 39.5 μM, we would predict approximately 40 to 70% inhibition of sulfadiazine hydroxylamine formation in vivo. Fluconazole has similar estimated apparent in vitro apparent IC_{50} and Ki estimates for inhibiting the production of hydroxylamine metabolites of two arylamine drugs, dapsone and sulfamethoxazole (Winter et al., 2000; Winter et al., 2004b). We have also shown that fluconazole can inhibit the in vivo hydroxylamine production of both dapsone and sulfamethoxazole by ~33 to 60% **(**Winter et al., 2004a; Winter et al., 2004b). On the basis of the above data, we predict that fluconazole, which is only 10% plasma protein bound, will substantially inhibit sulfadiazine hydroxylamine formation and may therefore be a clinical useful strategy to decrease adverse reactions to sulfadiazine in vivo**.** To test this strategy will require both an *in vivo* pharmacokinetic study to confirm significant inhibition of hydroxylamine production by fluconazole, followed by a larger clinical trial when fluconazole and sulfadiazine are chronically co-administered and the adverse effects of sulfadiazine are measured.

ACKNOWLEDGEMENTS: We would like to thank Tom Kalhorn, Department of Pharmaceutics, University of Washington, Seattle for his advice on hydroxylamine bioanalytical method development.

References

Atef M and Nielson P (1975) Metabolism of sulfadiazine in goats. *Xenobiotica* **5:**167-172.

Butcher NJ, Boukouvala S, Sim E and Minchin RF (2002) Pharmacogenetics of the arylamine N-acetyltransferases. *Pharmacogenomic J* **2**:30-42.

Grant DM, Blum M, Beer M, and Meyer UA (1991) Monomorphic and polymorphic human arylamine N-acetyltransferases: a comparison of liver isozymes and expressed products of two cloned genes. *Mol Pharmacol* **39:**184-191.

Gibbs MA, Thummel KE, Shen DD, and Kunze KL (1999) Inhibition of cytochrome P-450 3A (CYP3A) in human intestinal and liver microsomes: comparison of Ki values and impact of CYP3A5 expression. *Drug Metab Dispos* **27:**180-187.

Gill HJ, Tjia JF, Kitteringham NR, Pirmohamed M, Back DJ and Park BK (1999) The effect of genetic polymorphisms in CYP2C9 on sulfamethoxazole N-hydroxylation. *Pharmacogenetics* **9**:43-53.

Hansen JM, Kampmann JP, Siersbaek-Nielsen K, Lumholtz IB, Arroe M, Abildgaard U, and Skovsted L (1979) The effect of different sulfonamides on phenytoin metabolism in man. *Acta Med Scand* (Suppl) **624:**106-110.

Haverkos HW (1987) Assessment of therapy for toxoplasmic encephalitis. The TE study group. *Am J Med* **82:**907-914.

Hickman D, Wang J-P, Wang Y, and Unadkat JD (1998) Evaluation of the selectivity of *in vitro* probes and the suitability of organic solvents for the measurement of human cytochrome P450 monooxygenase activities. *Drug Metab Dispos* **26:**207-215.

Kirchheiner J, Brockmoller J, Meineke I, Bauer S, Rohde W, Meisel C and Roots I (2002) Impact of CYP2C9 amino acid polymorphisms on glyburide kinetics and on the insulin and glucose response in healthy volunteers. *Clin Pharmacol Ther* **71**:286-296.

Kunze KL, Wienkers LC, Thummel KE, and Trager WF (1996) Warfarin-fluconazole. I. Inhibition of the human cytochrome P450-dependent metabolism of warfarin by fluconazole: *in vitro* studies. *Drug Metab Dispos* **24:**414-421.

Leone N, Barzaghi N, Monteleone M, Perucca E, Cerutti R, and Crema A (1987) Pharmacokinetics of co-trimazine after single and multiple doses. *Arzneim Forsch/Drug Res* **37:**70-74.

Leport C, Raffi F, Matheron S, Katlama C, Regnier B, Saimot AG, Marche C, Vedrenne C, and Vilde JL (1988) Treatment of central nervous system toxoplasmosis with pyrimethamine/sulfadiazine combination in 35 patients with the acquired immunodeficiency syndrome. *Am J Med* **84:**94-100.

Levy RH (1995) Cytochrome P450 isozymes and antiepileptic drug interactions. *Epilepsia* **36(Suppl 5):**S8-13.

Miners JO, Smith KJ, Robson RA, McManus ME, Veronese ME, and Birkett DJ (1988) Tolbutamide hydroxylation by human liver microsomes: Kinetic characterization and relationship to other cytochrome P450 dependent xenobiotic oxidations. *Biochem Pharmacol* **37:**1137-1144.

Miners J (2002) CYP2C9 polymorphism: impact on tolbutamide pharmacokinetics and response. *Pharmacogenetics.* **12**:91-92.

Mitra AK, Thummel KE, Kalhorn TF, Kharash ED, Unadkat JD, and Slattery JT (1995) Metabolism of dapsone to its hydroxylamine by CYP2E1 *in vitro* and *in vivo*. *Clin Pharmacol Ther* **58:**556-566.

Mitra AK, Thummel KE, Kalhorn TF, Kharash ED, Unadkat JD, and Slattery JT (1996) Inhibition of sulfamethoxazole hydroxylamine formation by fluconazole in human liver microsomes and healthy volunteers. *Clin Pharmacol Ther* **59:**332-340.

Nouws JF, Firth EC, Vree TB, and Baakman M (1987) Pharmacokinetics and renal clearance of sulfamethazine, sulfamerazine, and sulfadiazine and their N4-acetyl and hydroxy metabolites in horses. *Am J Vet Res* **48:**392-402.

Nouws JF, Mevius D, Vree TB, Baakman M, and Degen M (1988) Pharmacokinetics, metabolism, and renal clearance of sulfadiazine, sulfamerazine and sulfamethazine and of their N4-acetyl and hydroxy metabolites in calves and cows. *Am J Vet Res* **49:**1059-1065.

Palamanda JR, Hickman D, Ward A, Sim E, Romkes-Sparks M, and Unadkat JD (1995) Dapsone acetylation by human liver arylamine N-acetyltransferases and interaction with anti-opportunistic infection drugs. *Drug Metab Dispos* **23:**473-477.

Rettie AE, Eddy AC, Heimark LD, Gibaldi M, and Trager WF (1989) Characteristics of warfarin hydroxylation catalyzed by human liver microsomes. *Drug Metab Dispos* **17:**265-270.

Rieder MJ, Uetrecht J, Shear NH, and Spielberg SP (1988) Synthesis and *in vitro* toxicity of hydroxylamine metabolites of sulfonamides. *J Pharmacol Exp Ther* **244**: 724-728.

Shaw PN and Houston JB (1987) Kinetics of drug metabolism inhibition: use of metabolite concentration-time profiles. *J Pharmacokinet Biopharm* **15:**497-510.

Shear NH and Spielberg SP (1985) *In vitro* evaluation of a toxic metabolite of sulfadiazine. *Can J Physiol Pharmacol* **63:**1370-1372.

Shon JH, Yoon YR, Kim KA, Lim YC, Lee KJ, Park JY, Cha IJ, Flockhart DA and Shin JG. (2002) Effects of CYP2C19 and CYP2C9 genetic polymorphisms on the disposition of and blood glucose lowering response to tolbutamide in humans. *Pharmacogenetics* **12**:111-119.

Veronese ME, Doecke CJ, MacKenzie PI, McManus ME, Miners JO, Rees DL, Gasser R, Meyer UA and Birkett DJ (1993) Site-directed mutation studies of human liver cytochrome P-450 isoenzymes in the CYP2C subfamily. *Biochem J* **289**:553-538.

Vree TB, Beneken Kolmer EW, and Peeters A (1991a) Comparison of the metabolism of four sulfonamides between humans and pigs. *Vet Q* **13:**236-240.

Vree TB, Vree JB, Beneken Kolmer EW, and Hekster YA (1991b) Novel oxidative pathways of sulfapyridine and sulfadiazine by the turtle *Pseudemys scripta elegans. Vet Q* **13:**218-224.

Vree TB, Schoondermark-van de Ven E, Verwey-van Wissen CP, Bars AM, Swolfs A, van Galen PM, and Amatdjais-Groenen H (1995) Isolation identification and determination of sulfadiazine and its hydroxy metabolites and conjugates from man and rhesus monkey by high-performance liquid chromatography. *J Chromatogra B Biomed* **670:**111-123.

Winter HR, Wang Y, and Unadkat JD (2000) CYP2C8/9 mediate dapsone N-hydroxylation at clinical concentrations of dapsone. *Drug Metab Dispos* **28:**865-868.

Winter HR, Trapnell CB, Slattery JT, Jacobson M, Greenspan DL, Hooton TM, and Unadkat JD (2004a) The effect of clarithromycin, fluconazole and rifabutin on dapsone hydroxylamine formation in individuals with human immunodeficiency virus infection (AACTG 283) *Clin Pharmacol Ther, 76*:579-587.

Winter HR, Trapnell CB, Slattery JT, Jacobson M, Greenspan DL, Hooton TM, and Unadkat JD (2004b) The effect of clarithromycin, fluconazole and rifabutin on sulfamethoxazole hydroxylamine formation in individuals with human immunodeficiency virus infection (AACTG 283) *Clin Pharmacol Ther* **76:**313-322.

Wolkenstein P, Carriere V, Charue D, Bastuji-Garin S, Revuz J, Bonjeau JC, Beaune P, and Bagot M (1995) A slow acetylator phenotype is a risk factor for sulfonamide-induced toxic epidermal necrolysis and Stevens-Johnson syndrome. *Pharmacogenetics* **5:**255-258.

Wrighton SA, Thomas PE, Willis P, Maines SL, Watkins PB, Levin W, and Guzelian PS (1987) Purification of a human liver cytochrome P-450 immunochemically related to several cytochromes P-450 purified from untreated rats. *J Clin Invest* **80:**1017-1022.

FOOTNOTES

Supported in part by NIGMS grant P01GM32165.

Reprint requests:

Jashvant D. Unadkat

Department of Pharmaceutics, Box 357610, University of Washington, Seattle WA 98195 USA

Fax: (206) 543-3204 Tel: (206) 543-9434

EMAIL: jash@u.washington.edu

LEGENDS TO FIGURES

Fig. 1. Chromatograms showing (a) UV absorbance at λ=266 nm (and retention times) of aqueous standards of the oxidative metabolites of sulfadiazine (50 ng injected on column)- 4-hydroxy sulfadiazine (8.4 min), N4-hydroxy sulfadiazine (10.2 min), 5-hydroxy sulfadiazine (11.9 min), and sulfadiazine (12.8 min); (b) electrochemical (EC) tracing (R = 100 nA, attenuation 5) showing formation of 135 pmol hydroxylamine/mg microsomal protein in a 10 min microsomal incubation containing 200 μM sulfadiazine and 1 mM NADPH; (c) EC tracing of microsomal blank for 200 μM sulfadiazine. Chromatograms were recorded on a Shimadzu Chromatopac CR601.

Fig. 2. Eadie-Hofstee plots for N-hydroxylation of sulfadiazine (SDZ-HA) in human liver microsomes over the range 300 μM to 10 mM. The average Km (± SD, n = 3) and Vmax, estimated by nonlinear regression, were 5.7 ± 2.2 mM and 185 ± 142 pmol/min/mg protein, respectively.

Fig. 3. Isoform specific inhibition of hydroxylamine formation in HL141 at 100 μM sulfadiazine. Isoform specificities were tolbutamide = CYP2C8/9, sulfaphenazole = CYP2C9, caffeine = CYP1A2, chloroxazone = CYP2E1, ρ-nitrophenol = CYP2E1, troleandomycin = CYP3A4, quinidine = 2D6, coumarin = 2A6, S-mephenytoin = CYP2C19, and orphenadrine = CYP2B6. All inhibitors were compared with solvent matched controls containing not more than 0.3% solvent. Data are presented as mean and standard deviation of triplicate observations.

Fig. 4. The rate of sulfadiazine hydroxylamine (SDZ-HA) formation (4 mM sulfadiazine) is significantly correlated (r = 0.76, $p \leq 0.004$; r_s = 0.78, $p < 0.002$) with CYP2C8/9 activity (4-hydroxylation of 500 μM tolbutamide) in 12 human livers.

Fig. 5. Lineweaver Burk (upper) and Dixon (lower) plots for fluconazole inhibition of sulfadiazine hydroxylamine (SDZ-HA) formation in HL142 (left panel) and HL123 (right panel). The Ki values for one-enzyme models of fluconazole inhibition were determined to be (mean ± SEM) 8.6 ± 0.6 μM in HL142 (apparent competitive mechanism) and 39.5 ± 2.8 μM in HL123 (apparent noncompetitive mechanism).

Fig. 6. Eadie-Hofstee plots for N-acetylation of sulfadiazine (AcSDZ) in human liver cytosol over the range 156 μM to 5 mM. The average Km (± SD) and Vmax were determined to be 3.1 ± 1.7 mM and 221.8 ± 132.3 pmol/min/mg protein at an acetyl coenzyme A concentration of 100 μM.

Fig. 7. Isoform specific inhibition of N-acetyl sulfadiazine formation in human liver cytosol at 50 μM and 1000 μM sulfadiazine (SDZ). Probe specificities were ρ-aminobenzoic acid (PABA) = NAT1 and sulfamethazine (SMZ) = NAT2. N.D. = not detectable

Fig. 8. a) Lack of correlation between the rate of acetylation of 5 mM sulfadiazine with NAT1 activity (Vmax for acetylation of ρ-aminobenzoic acid) in 12 human livers (r = -0.12, p = 0.74). b) Highly significant correlation between the rate of acetylation of 5 mM sulfadiazine with NAT2 activity (Vmax for acetylation of sulfamethazine) in 12 human livers (r = 0.96, $p \leq 0.001$; r_s = 0.93, $p \leq 0.001$).

Table 1. Wild type recombinant NAT1 and NAT2 enzyme kinetic parameters for acetylation of para amino benzoic acid, sulfadiazine, and sulfamethazine

Enzyme	**Substrate**	**Vmax**	**Km**
NAT1*3#	Para amino benzoic acid (PABA)	6.4 nmol/min/mg	687 μM
NAT1*3	Sulfadiazine	18.3 nmol/min/mg	5.8 mM
NAT2*4#	Sulfamethazine (SMZ)	0.8 nmol/min/mg	136 μM
NAT2*4	Sulfadiazine	2.98 nmol/min/mg	5.4 mM

[#]We used exactly the same source of cloned NAT enzyme, within a similar time frame as reported by Palamanda JR, Hickman D, Ward A, Sim E, Romkes-Sparks, and Unadkat JD *Drug Metabolism and Disposition* (1995) 23(4):473-477.

DMD Fast Forward. Published on April 20, 2005 as DOI: 10.1124/dmd.104.002998
This article has not been copyedited and formatted. The final version may differ from this version.

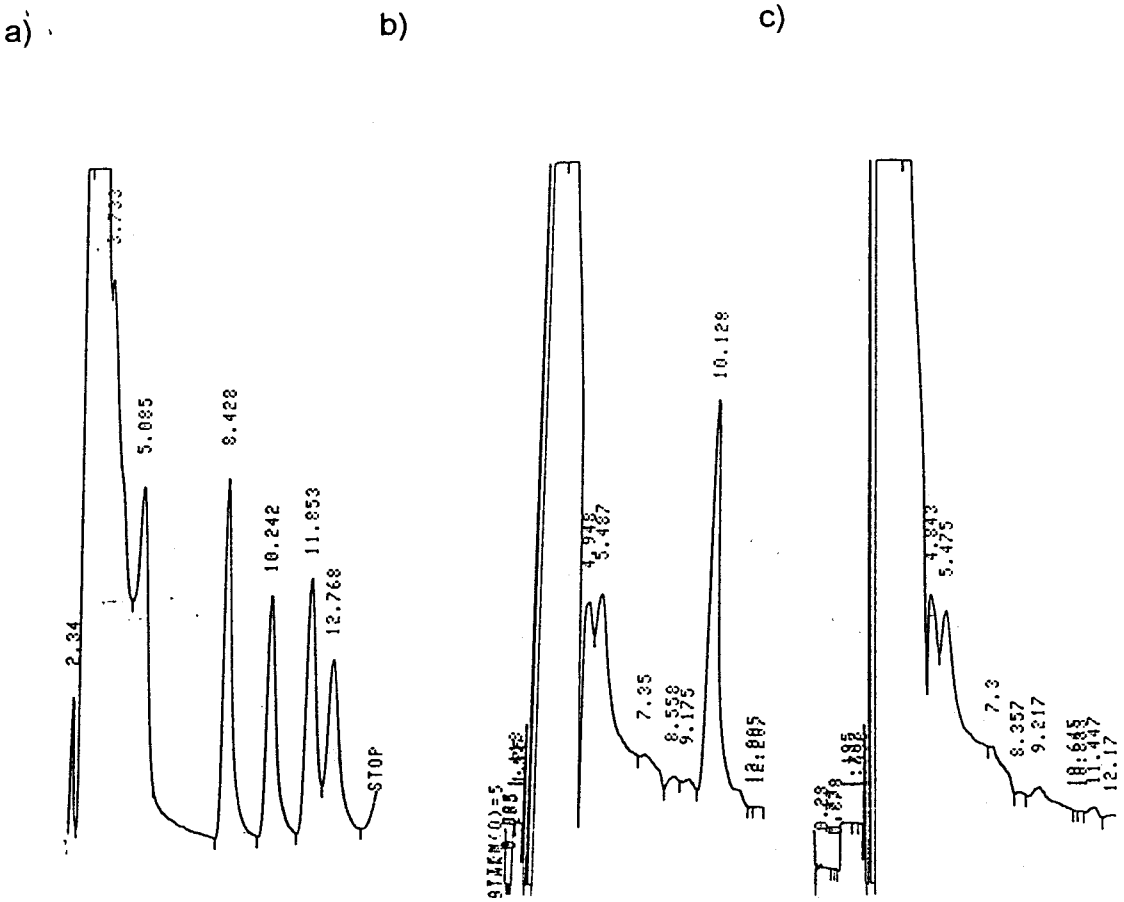

Fig. 1

DMD Fast Forward. Published on April 20, 2005 as DOI: 10.1124/dmd.104.002998
This article has not been copyedited and formatted. The final version may differ from this version.

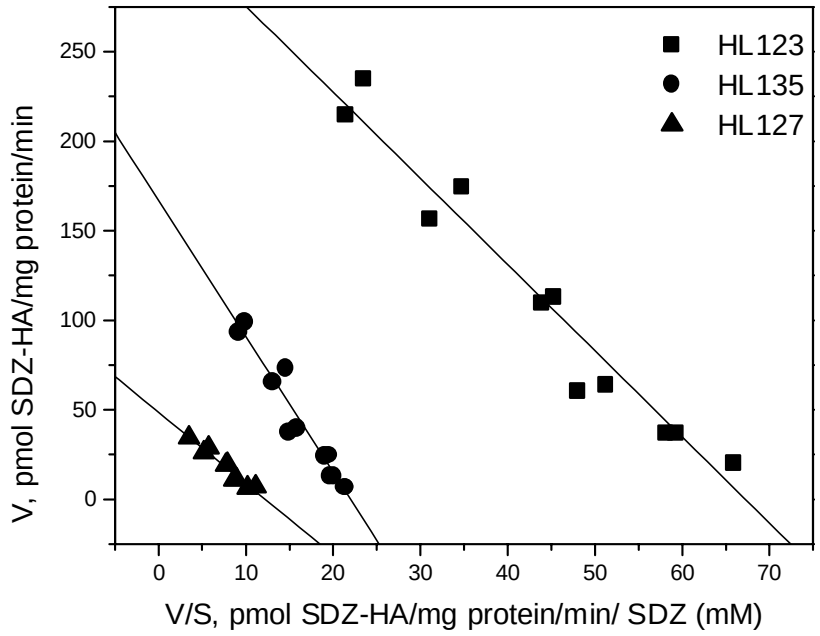

Fig. 2

DMD Fast Forward. Published on April 20, 2005 as DOI: 10.1124/dmd.104.002998
This article has not been copyedited and formatted. The final version may differ from this version.

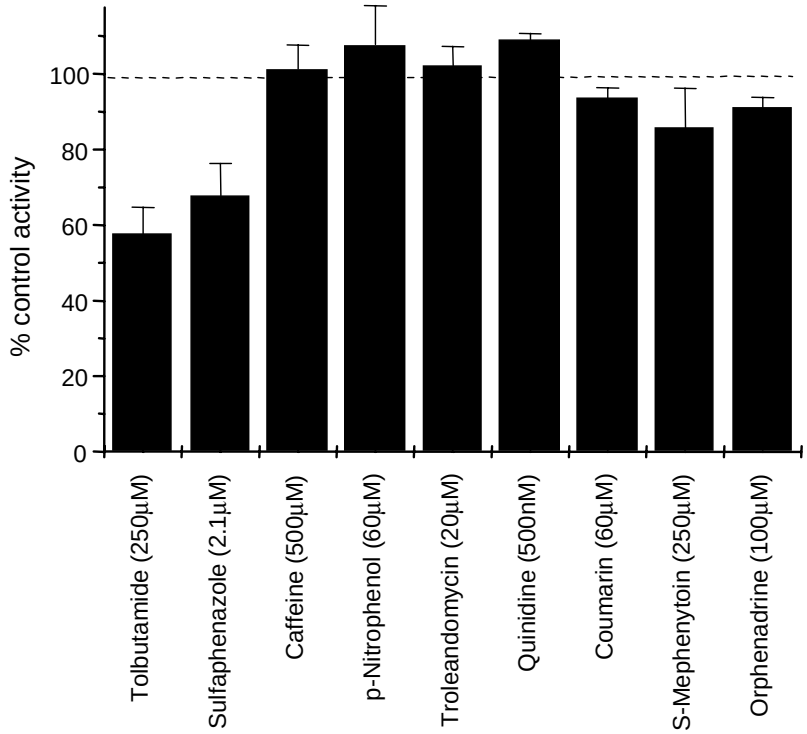

Fig. 3

DMD Fast Forward. Published on April 20, 2005 as DOI: 10.1124/dmd.104.002998

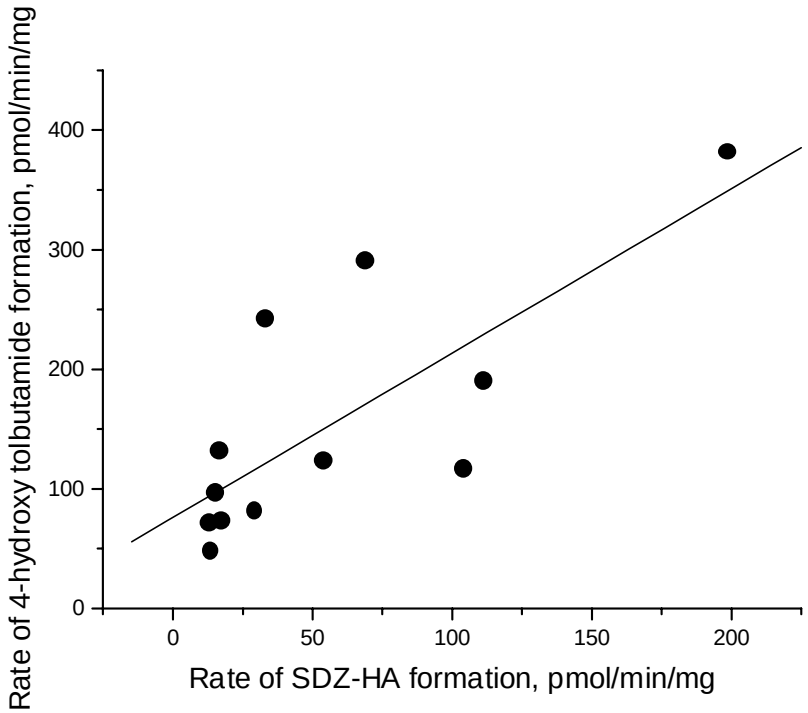

Fig. 4

DMD Fast Forward. Published on April 20, 2005 as DOI: 10.1124/dmd.104.002998
This article has not been copyedited and formatted. The final version may differ from this version.

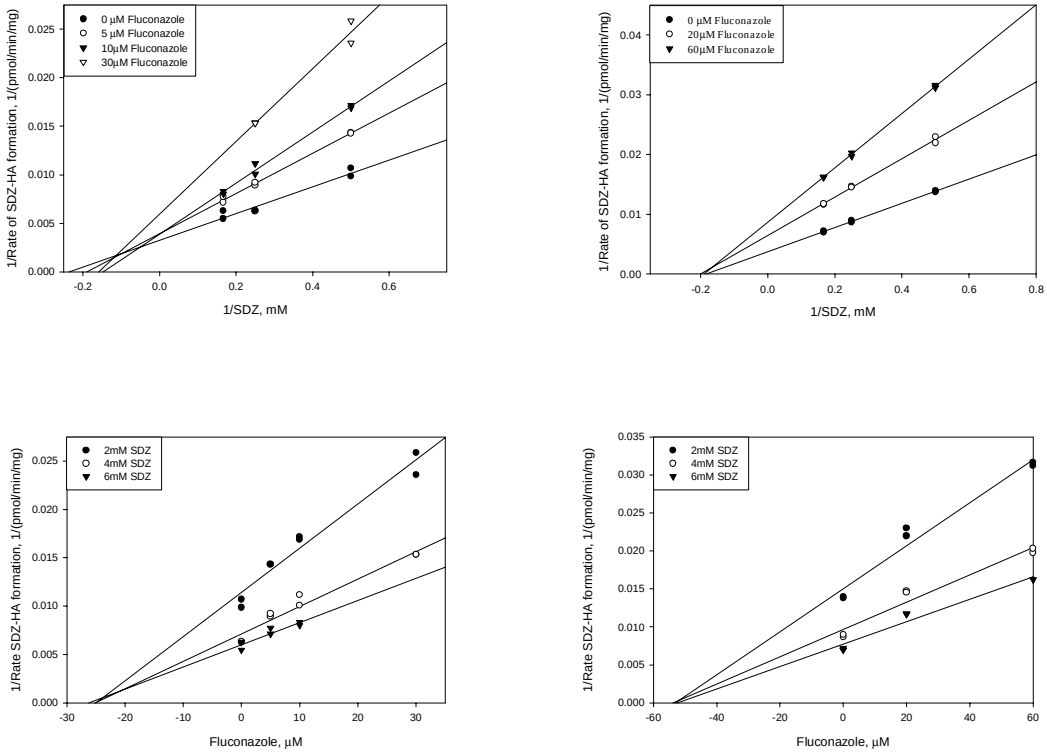

Fig. 5

DMD Fast Forward. Published on April 20, 2005 as DOI: 10.1124/dmd.104.002998
This article has not been copyedited and formatted. The final version may differ from this version.

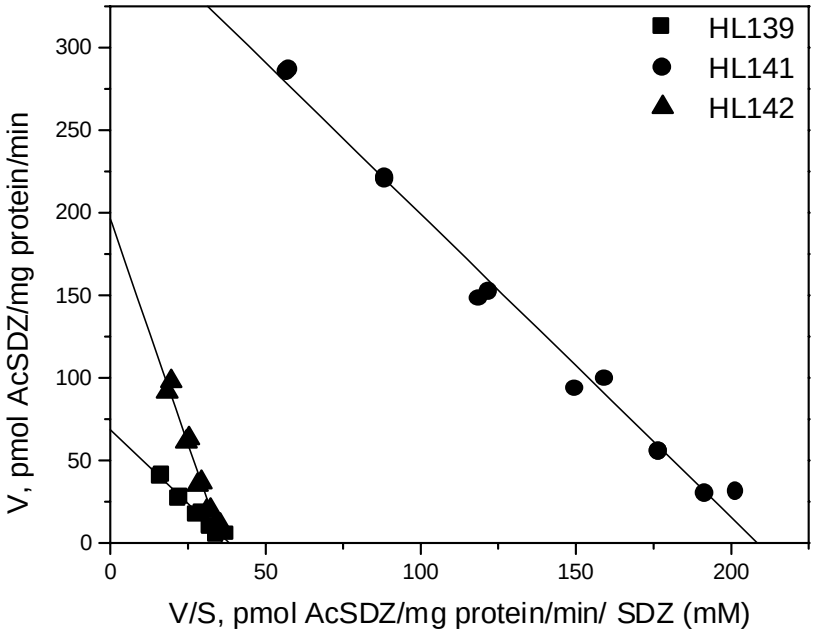

Fig. 6

DMD Fast Forward. Published on April 20, 2005 as DOI: 10.1124/dmd.104.002998
This article has not been copyedited and formatted. The final version may differ from this version.

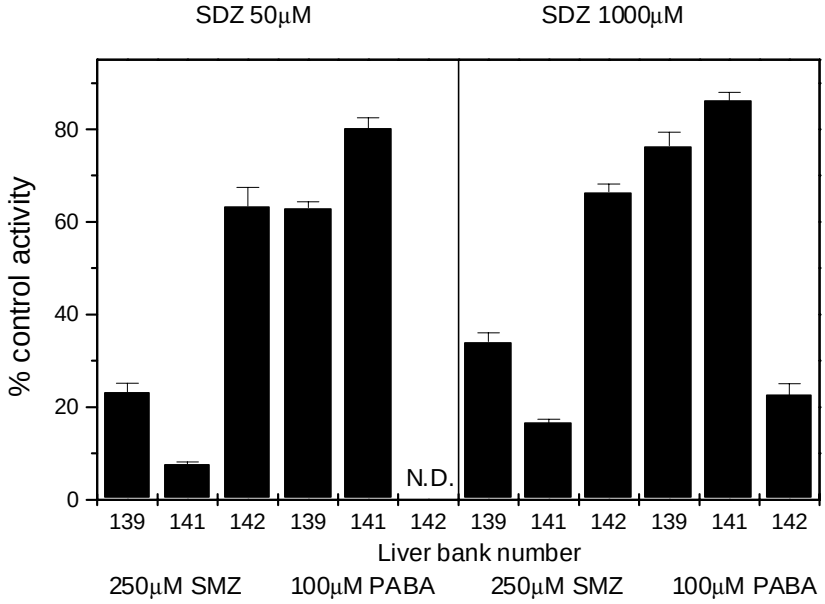

Fig. 7

DMD Fast Forward. Published on April 20, 2005 as DOI: 10.1124/dmd.104.002998
This article has not been copyedited and formatted. The final version may differ from this version.

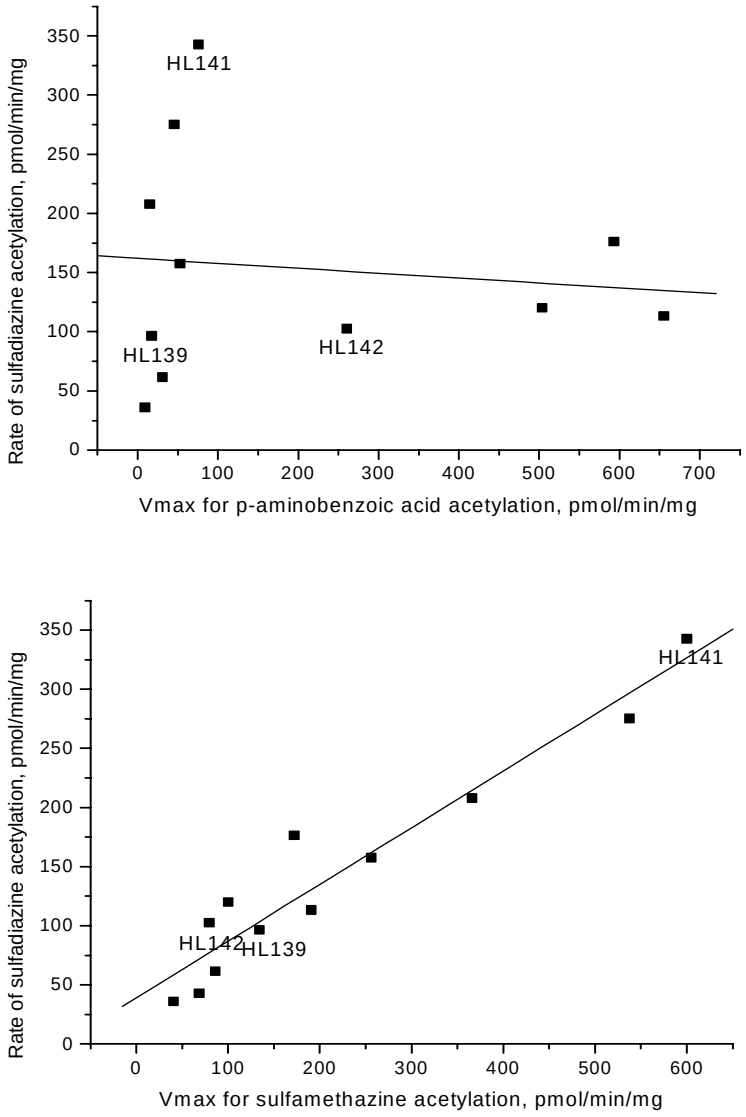

Fig. 8